Phonon-Wind–Driven Electron-Hole Plasma in Si

F. M. Steranka and J. P. Wolfe
Physics Department and Materials Research Laboratory, University of Illinois at Urbana-Champaign, Urbana, Illinois 61801
(Received 3 April 1984)

The spatial expansion of electron-hole plasma created by nanosecond pulsed-laser excitation of Si is examined by time-resolved luminescence imaging. On a several-nanosecond time scale, the plasma created by 0.5-μJ excitation expands from the excitation point at subsonic velocities, contrary to a fast-diffusing plasma model recently proposed to explain spectroscopic anomalies. For 50-μJ excitation, time-resolved images show a shell of plasma expanding at near-sonic velocities, indicating phonon-wind–driven transport with highly nonlinear damping.

PACS numbers: 71.35.+z, 72.20.Ht

Intense laser excitation of a semiconductor produces a plasma of electrons and holes. These hot photoexcited carriers approach the lattice temperature on a subnanosecond time scale, as demonstrated in recent reflectivity and absorption experiments with picosecond laser pulses.[1] A large group of experiments, e.g., those involving pulsed-laser annealing, employ pulse widths in the $\sim$10- to 100-ns range, and the evolution of the electronic and thermal energy following such excitation is the subject of much interest and controversy. Radically different predictions concerning the motion of the electron-hole plasma have been forwarded. On one hand, it has been suggested that the plasma produced by nanosecond pulses will be confined near the excitation surface, aiding in the annealing process.[2] Another viewpoint,[3] based on recombination luminescence spectra, is that at low temperatures the plasma rapidly diffuses into the crystal at a velocity comparable to its Fermi velocity, i.e., in the range 10^6 to 10^7 cm/s. In the present Letter, we report the first spatial measurements of the plasma expansion process in silicon. Our principal results are that, on a several-nanosecond time scale, the plasma generated at the surface of the crystal is neither stationary nor fast diffusing and that an intense flux of nonequilibrium phonons provides the dominant driving force.

Spectroscopy has proven to be a valuable tool in the characterization of solid-state plasma. Recombination of electron-hole pairs in the plasma produces a broad luminescence spectrum characteristic of a Fermi distribution of kinetic energies [see Fig. 1(a)]. The width of the spectrum is related to the Fermi energy and, thus, to the density of the particles. Mahler *et al.*[4] argued that the plasma created by intense surface excitation of Si is composed of carriers at nearly a single density, implying that the luminescence emission line may be fitted by means of a single Fermi energy. Later, Forchel and coworkers[3] pointed out that the plasma density obtained in this way was not consistent with the spectral position of the plasma luminescence. It is well known that the semiconductor energy gap, which determines the energy position of the plasma spectrum, is reduced in the presence of a high density of carriers, as a result of Coulomb interactions. This "renormalization gap" has been calculated[5,6] as a function of density, and the density derived from the spectral position of the plasma luminescence is considerably smaller than that derived from the width of the spectrum. To explain this anomaly, Forchel and co-workers[3] proposed that the carriers in the plasma were drifting away from the excitation point at a velocity comparable to the Fermi velocity. For a given density, a "drifted" Fermi distribution produces a broader range of kinetic energies than would an equilibrium distribution and leads to a broader luminescence spectrum. They argued that a wide variety of highly excited semiconductors (e.g., Si, Ge, GaAs, CdS, and ZnSe) exhibited such fast diffusing electron-hole plasmas. Previous[7] and subsequent[8] studies of e-h plasmas in direct-gap semiconductors also indicate very high drift velocities, of order 10^7 cm/s.

To observe the plasma expansion process in Si directly, we have combined time-resolved spectroscopy with spatial imaging. The luminescence was detected with an infrared-sensitive phototube, and single-photon counting allowed 5-ns temporal resolution. Syton-polished crystals of ultrapure silicon ($N_A - N_D < 10^{12}$ cm^{-3} from Siemens) were cooled to temperatures between 2 and 50 K in an optical cryostat. A cavity-dumped Ar^+ laser beam, with pulses of 8-ns full width and up to 0.5-μJ incident energy, was focused to a 30-μm-diam spot on the crystal. Spectra were obtained with a $\frac{1}{2}$-m spectrometer, and spatial profiles of the luminescence were achieved by the scanning of a 4×-magnified image of the crystal across a narrow (120 μm) spectrometer entrance slit.

Time-resolved spectra for a crystal at $T = 25$ K

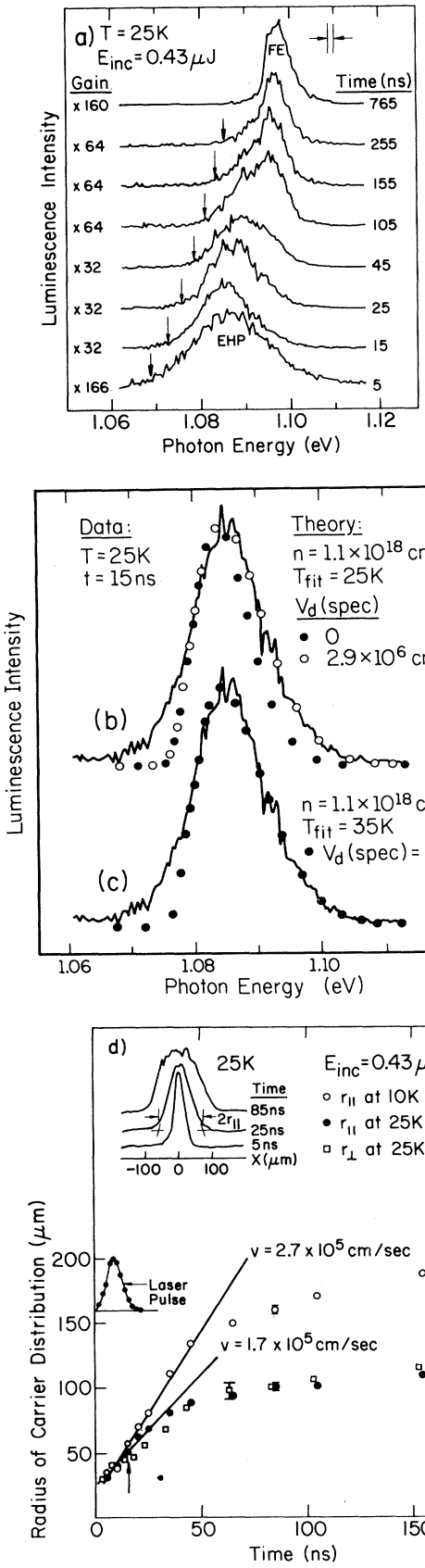

FIG. 1. (a) Time-resolved spectra at $T = 25$ K. A 5-ns time gate was used for the first 30 ns and, to optimize the signal, was gradually opened to 50 ns at later times. The arrows indicate the position of the low-energy edge of the plasma luminescence. (b) Fit to the 15-ns spectrum from (a) using drifted Fermi functions and the lattice temperature (25 K). (c) Fit to the 15-ns spectrum from (a) with $T = 35$ K. (d) Radii of the carrier distribution parallel ($r_{\parallel}$) and perpendicular ($r_{\perp}$) to the crystal surface vs time. Both EHL, at 10 K, and EHP, at 25 K, are shown. The inset shows time-resolved slit scans of EHP looking into the laser beam direction. The arrow indicates the time at which the spectrum in (b) and (c) was recorded.

are shown in Fig. 1(a). A broad luminescence peak characteristic of a dense electron-hole plasma[9] (EHP) appears during the laser pulse (between 0 and 20 ns) and continuously narrows and shifts to higher energy with time. At times exceeding about 50 ns, a free-exciton component appears and remains well after the plasma has disappeared. The shift of the low-energy edge of the EHP spectrum [arrows in Fig. 1(a)] indicates that the density decreases with time. In Fig. 1(b) we compare drifted and undrifted theoretical curves to the plasma spectrum at $t = 15$ ns, assuming consistency between the plasma density and renormalized gap[6] and a plasma temperature equal to the lattice temperature. As Forchel and co-workers found, the assumption of a drifted Fermi distribution greatly improves the agreement with the data, here yielding a drift velocity of 2.9×10^6 cm/s.

The actual expansion rate of the plasma is determined from the time-resolved spatial profiles of the luminescence, as plotted in the inset of Fig. 1(d). The initial full width is consistent with our measured spatial resolution and laser spot size. A 3-meV spectral window centered at 1.090 eV was chosen for these measurements, but the resultant radii were independent of this choice of photon energy within the plasma emission. The initial expansion velocity and final penetration depth were dependent, however, on laser power. The velocity $v = 1.7 \times 10^5$ cm/s is representative of the average rate of expansion during the 20 ns following the start of the 0.43-μJ laser pulse. This velocity was about the highest obtainable with the cavity-dumped laser source. The plasma expansion is actually slower than that observed for the electron-hole liquid (EHL), obtained at lower temperature (10 K). We believe that this is due to a decrease in momentum relaxation time with increasing temperature.[10]

Clearly, the spectroscopic analysis which assumes

a drifted Fermi distribution yields a drift velocity which is inconsistent with the observed spatial expansion. Indeed, if the plasma were drifting at 2.9×10^6 cm/s for the 20-ns duration of the laser pulse, the radius of the plasma distribution would be nearly 600 μm at the end of the pulse. What then is the cause of the broadening in the spectrum? Spatial inhomogeneity of the plasma density is a likely contributor: The long low-energy tail of the spectrum probably indicates a region of higher plasma density. Another probable contributor to the spectral linewidth is a local heating of the lattice and plasma at early times. Figure 1(c) shows good agreement between the same spectrum at $t=15$ ns and an undrifted theory with $T=35$ K, which is 10 K above the bath temperature. Similar thermal effects have been reported by Shah and Dayem[9] for EHL at 1.8 K. In our case, a 10-K lattice heating over the measured plasma volume is consistent with the energy deposited by the laser.

To gain further insight into the plasma-expansion process, we have performed time-resolved imaging experiments at much higher laser energies. A nitrogen laser beam ($\lambda=337$ nm) focused to a spot of 600×100 μm^2 dimension and up to 53 μJ of incident energy produces a plasma of similar maximum density (about a factor of 2 greater) but which expands much further into the sample. This maximum energy is close to the damage threshold of the crystal. By adding a crossed slit to the spectrometer and raster scanning the image of the crystal across this aperture, we have obtained images of the luminescence as shown in Fig. 2. The plasma is seen to expand as a shell into the crystal. This striking behavior indicates that the plasma is *driven* from the excitation region, rather than simply diffusing.

We observe the same qualitative behavior for EHL; the droplets move as an expanding shell from the excitation spot (see the inset in Fig. 3). Previous experiments[11,12] have shown that the driving force on the droplets is provided by a ballistic flux of nonequilibrium phonons which are created at the excitation surface by hot-carrier thermalization. The similarities between the EHL and EHP images imply that the primary driving force in the EHP expansion is also the phonon wind. In fact, as is shown in Fig. 3, the initial expansion velocity varies continuously from temperatures below the EHL critical temperature, $T_c\approx22$ K, up to 50 K—further evidence that the transport mechanism is the same for both EHL and EHP. We note that the effects of ballistic phonons are not included in the previous thermodiffusion[4] and hydrodynamic[13] models for plasma expansion.

Another interesting feature of the measured expansion velocities shown in Fig. 3 is the abrupt saturation at $v=5.1\times10^5$ cm/s that occurs as the crystal temperature is lowered below 10 K, even though the momentum-damping rate due to carrier-phonon scattering continues to decrease as the temperature is lowered.[10] Certainly, the transverse phonons become less effective at pushing the droplets once the droplet velocity approaches the transverse sound velocity. However, the longitudinal phonons have velocities up to twice those of the transverse phonons and should be capable of exerting large forces on the droplets even when they are moving at velocities near the transverse sound velocity. We conclude that a

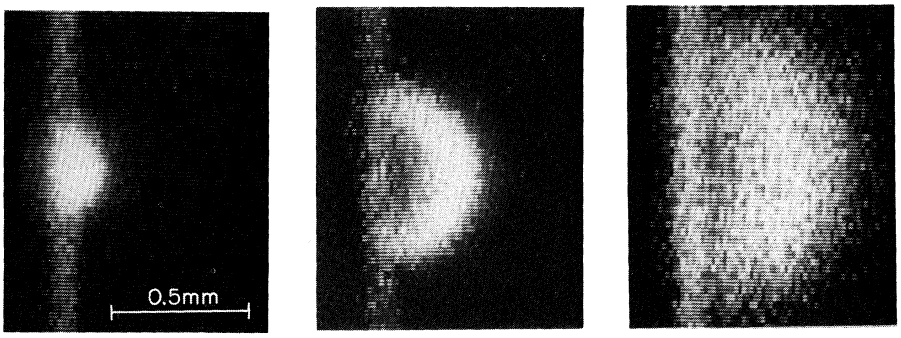

FIG. 2. Time-resolved images at $T=32$ K following excitation with a pulsed N_2 laser. The laser is incident from the left and the white vertical line is luminescence light scattered from the crystal surface. Images (a) and (b) show the EHP expanding as a shell from the excitation spot ($h\nu=1.090$ eV). Excitons are observed to move into the crystal with the EHP, and they diffuse to greater distances once the plasma has dissipated (≈800 ns). Image (c) shows the free-exciton ($h\nu=1.098$ eV) distribution 3 μs after the laser pulse. Spectral resolution is 3.5 meV. Spatial resolution is 120 μm. Temporal resolution is (a) 25 ns, (b) 50 ns, and (c) 200 ns.

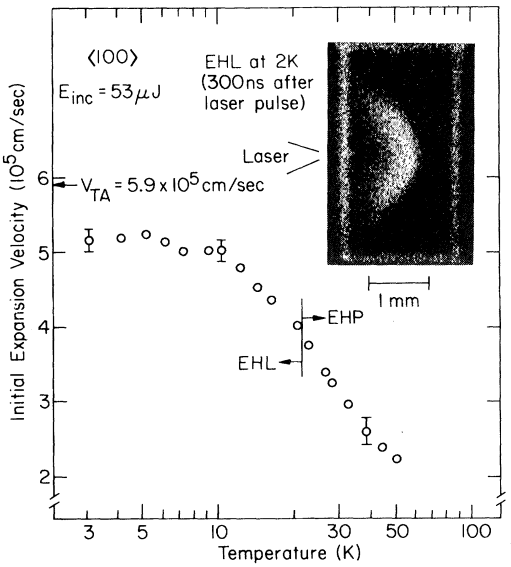

FIG. 3. Initial expansion velocity, obtained from slit scans with 10-ns and 60-μm resolution, vs crystal temperature following excitation with a pulsed N_2 laser. Velocities measured below 22 K correspond to EHL while those measured above 22 K correspond to EHP. The inset is a time-resolved image of the expanding EHL shell at $T = 2$ K. The entire $1.7 \times 2.9 \times 3.0$ mm^3 crystal is shown.

strong damping mechanism is turning on at 5.1×10^5 cm/s—possibly a Cherenkov-type emission[14] of TA phonons from the EHL that is preventing the droplets from reaching supersonic velocities. A velocity saturation effect at $v = 5.1 \times 10^5$ cm/s has also been observed in EHL drift experiments.[10]

In conclusion, by using time-resolved luminescence-imaging techniques, we have performed the first direct spatial measurements of the EHP expansion process in Si. We find that, on a several-nanosecond time scale, the average expansion velocity of the EHP is subsonic—contrary to recent claims based on spectral information. Local heating and inhomogeneous plasma density are the most probable contributors to the anomalously broad spectral line shapes. Under near-annealing excitation levels, the EHP is driven as a shell into the crystal by an intense phonon-wind force. At low temperatures ($T < 10$ K) and high excitation levels, we observe a saturation in the EHL expansion velocity at $v = 5.1 \times 10^5$ cm/s. Thus, our results show that a realistic theoretical description of plasma expansion at low temperatures must include the effects of ballistic phonon flux and nonlinear momentum damping at near-sonic drift velocities.

This work was supported in part by the National Science Foundation through the Materials Research Laboratory Grant No. NSF DMR-80-20250. Equipment support (laser sources) was provided under Grants No. NSF DMR-80-24000 and AFOSR-79-0124. We thank A. Mysyrowicz for helpful comments.

[1]C. V. Shank, R. Yen, and C. Hirlimann, Phys. Rev. Lett. **50**, 454 (1983); C. V. Shank, R. L. Fork, R. F. Leheny, and Jagdeep Shah, Phys. Rev. Lett. **42**, 112 (1979).

[2]M. Wautelet and J. A. Van Vechten, Phys. Rev. B **23**, 5551 (1981).

[3]A. Forchel, H. Schweitzer, and G. Mahler, Phys. Rev. Lett. **51**, 501 (1983); B. Laurich and A. Forchel, in *Energy Beam Solid Interactions and Transient Thermal Processes,* edited by J. C. C. Fan and N. M. Johnson, Materials Research Society Symposium Proceedings Vol. 23 (North-Holland, Amsterdam, 1984), p. 75; A. Forchel, H. Schweizer, B. Laurich, and G. Tränkle, *ibid.,* p. 209.

[4]G. Mahler, G. Maier, A. Forchel, B. Laurich, H. Sanwald, and W. Schmid, Phys. Rev. Lett. **47**, 1855 (1981).

[5]J. C. Hensel, T. G. Phillips, G. A. Thomas, and T. M. Rice, in *Solid State Physics: Advances in Research and Applications,* edited by H. Ehrenreich, F. Seitz, and D. Turnbull (Academic, New York, 1977), Vol. 32.

[6]P. Vashishta and R. Kalia, Phys. Rev. B **25**, 6492 (1982).

[7]K. M. Romanek, H. Nather, J. Fischer, and E. O. Gobel, J. Lumin. **24/25**, 585 (1981); S. Modesti, L. G. Quagliano, and A. Frova, J. Lumin. **24/25**, 581 (1981).

[8]K. Kempf and C. Klingshirn, Solid State Commun. **49**, 23 (1984).

[9]Jagdeep Shah and A. H. Dayem, Phys. Rev. Lett. **37**, 861 (1976).

[10]M. A. Tamor and J. P. Wolfe, Phys. Rev. B **26**, 5743 (1982).

[11]M. A. Tamor and J. P. Wolfe, Phys. Rev. B **21**, 739 (1980).

[12]M. Greenstein and J. P. Wolfe, Phys. Rev. B **24**, 3318 (1981); M. A. Tamor, M. Greenstein, and J. P. Wolfe, Phys. Rev. B **27**, 7353 (1983).

[13]M. Combescot, Solid State Commun. **30**, 81 (1979).

[14]A. V. Subashiev, Fiz. Tverd. Tela (Leningrad) **22**, 738 (1980) [Sov. Phys. Solid State 22, 431 (1980)], and references therein.

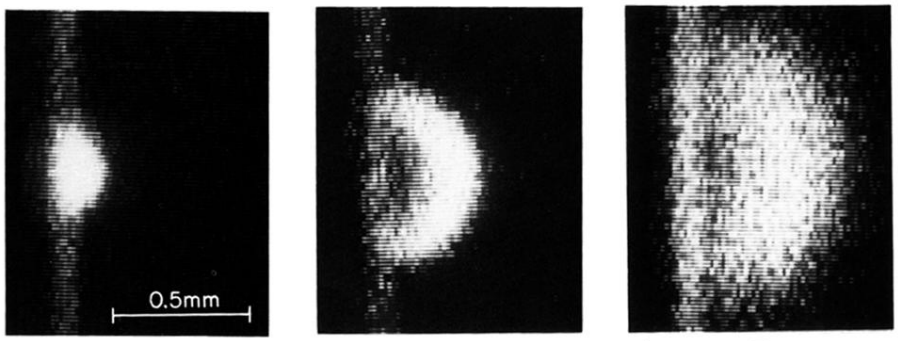

FIG. 2. Time-resolved images at $T = 32$ K following excitation with a pulsed N_2 laser. The laser is incident from the left and the white vertical line is luminescence light scattered from the crystal surface. Images (a) and (b) show the EHP expanding as a shell from the excitation spot ($h\nu = 1.090$ eV). Excitons are observed to move into the crystal with the EHP, and they diffuse to greater distances once the plasma has dissipated (≈ 800 ns). Image (c) shows the free-exciton ($h\nu = 1.098$ eV) distribution 3 μs after the laser pulse. Spectral resolution is 3.5 meV. Spatial resolution is 120 μm. Temporal resolution is (a) 25 ns, (b) 50 ns, and (c) 200 ns.

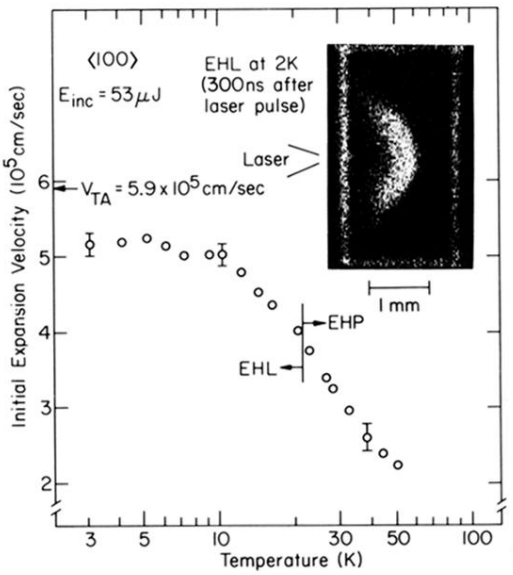

FIG. 3. Initial expansion velocity, obtained from slit scans with 10-ns and 60-μm resolution, vs crystal temperature following excitation with a pulsed N_2 laser. Velocities measured below 22 K correspond to EHL while those measured above 22 K correspond to EHP. The inset is a time-resolved image of the expanding EHL shell at $T = 2$ K. The entire $1.7 \times 2.9 \times 3.0$ mm^3 crystal is shown.